Supplementary materials for Genaev et al. “Morphometry of the Wheat Spike by Analyzing 2D Images”

File content:

1. Protocol for Image Capture

1.1. ‘Clip’ protocol

Spike and ColorChecker were fixed with clips in front of a blue paper background. Rotation of the spike around its axis allows the images to be captured in several projections. Two pulsed light sources, Falcon DE-300 (flash intensity, 2.5), Falcon 60 × 60 soft boxes as light modifiers, and a Canon 350D digital camera with an EF-S 18-55mm f/3.5-5.6 lens were used. Shooting settings: shutter speed, 1/160; aperture, 11; ISO 100; focal lens, 55 mm; and RAW format; white balance was set according to the ColorChecker white background when developing a RAW file. The distance from spike to background was 60 cm; to light sources, 100 cm; and to camera, 120 cm. The camera mounted on a tripod, spike, and light sources were at the same height comfortable for photographer’s work.

Figure S1 shows the layout of camera and light sources relative to the object and the resulting image captured according to the protocol.

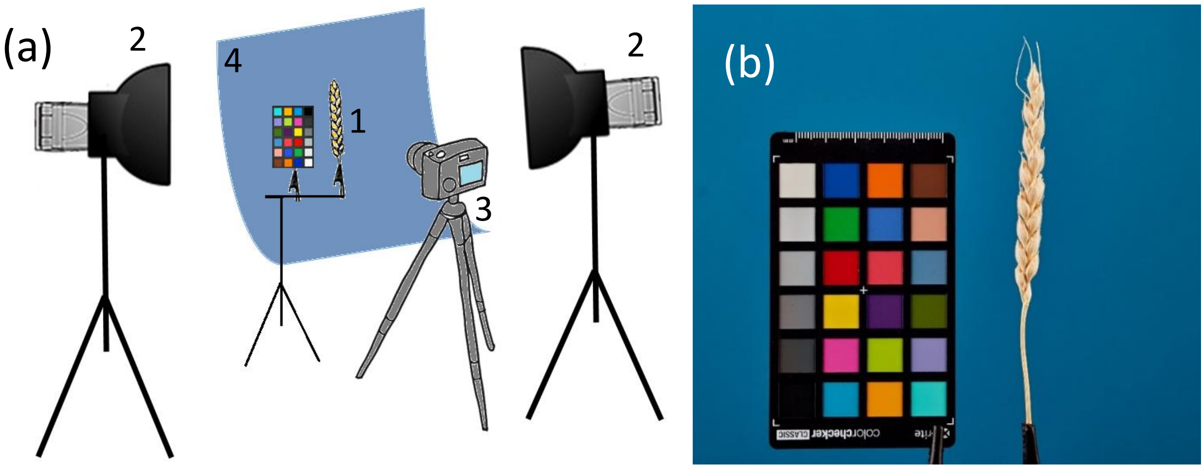

Figure S1. ‘Clip’ protocol. (a) Layout of camera and light sources relative to the object: 1, spike; 2, light sources; 3,- camera; and 4, paper background. (b) An example the image taken according to the ‘clip’ protocol.

1.2 ‘Table’ Protocol

In this variant, the captured spike is placed onto a transparent sample stage on a table with a blue surface (background). The camera is mounted above the transparent sample stage on a tripod with a boom arm. Two pulsed light sources, Falcon DE-300 (flash intensity, 1.0 and 1.4), Falcon 60 × 60 soft boxes as light modifiers, and Canon 600D digital camera with an EF-S 28-135mm f/3.5-5.6 lens were used. Shooting settings: shutter speed, 1/160; aperture, 10; ISO 200; focal lens, 112 mm; and RAW format; white balance was set according to the ColorChecker white background when developing a RAW file. The distance of the camera to the object was 70 cm; of the light sources to the object, 60 cm; table height, 60 cm; and the height of the transparent sample stage (the distance of the object to blue background), 20 cm.

Layout of the camera and light sources relative to the object and an image captured according to this protocol are shown in Figure S2.

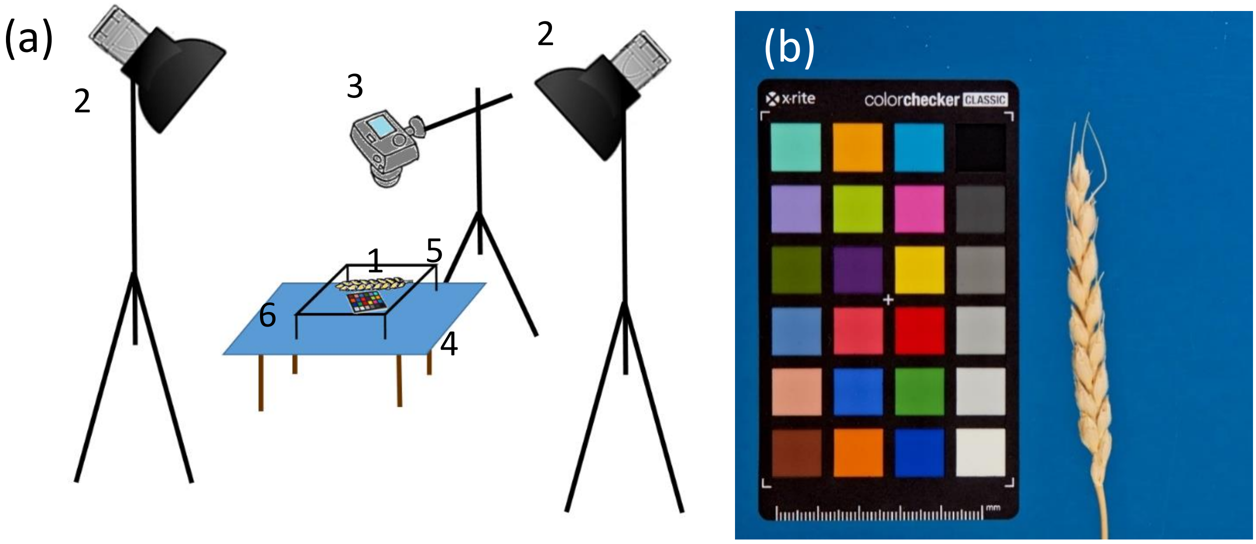

Figure S2. 'Table' protocol. (a) Layout of the camera and light sources relative to the object: 1, spike; 2, light sources; 3, camera; 4, subject table; 5, transparent sample stage; and 6, paper background. (b) An example of the image taken according to the 'table' protocol.

2. Algorithm for Color Scale Identification

2.1 Identifying Color Scale

The ColorChecker scale is identified by comparing it in a calibratable image (spike image) to a reference image. Initially, key points are found in the calibrated image using ORB algorithm (Oriented FAST and Rotated BRIEF, Feature2D::detect method; see the manual to OpenCV library, https://opencv.org, [1]). The key points are transformed to a form invariant relative to scaling and rotation, i.e., descriptors (Feature2D::extract). Each descriptor is a numerical vector.

Then, two descriptors of the calibrated image closest in the Hamming distance ($firstDescriptor$ and $secondDescriptor$) are selected for each descriptor of the reference image ($refDescriptor$) using DescriptorMatcher::knnMatch method. The pairs of ($refDescriptor$, $firstDescriptor$) type that meet the below condition are selected from the obtained pairs:

$$distance[refDescriptor, firstDescriptor] < threshold\_of\_distance[refDescriptor, secondDescriptor]$$

The following projective transformation between the key points is constructed according to the obtained pairs of descriptors with the help of RANSAC algorithm implemented Calib3d.findHomography:

$$\begin{bmatrix} x' \\ y' \\ 1 \end{bmatrix} = \begin{bmatrix} h_{11} & h_{12} & h_{13} \\ h_{21} & h_{22} & h_{23} \\ h_{31} & h_{32} & h_{33} \end{bmatrix} \begin{bmatrix} x \\ y \\ 1 \end{bmatrix}$$

The transformation is applied to the known angles of the reference image; this gives the angles of the region that contained the color scale on the calibrated image (Core.perspectiveTransform). The region is cut off from the image and is rotated so to match the reference image.

The scale of image (pixel size in mm) is computed from the ratio of the known color scale area and its area in the image (taking into account the correction for orientation).

2.2. Correcting Colors

The image color was calibrated with the color correction method used in epiluminescence [2].

Nine points are selected in each square of the palette in the cut-off and rotated image to be used in further calibration. For each point, the feature vector is constructed using one of the polynomial regression methods:

$x = [R\ G\ B]$ (1)

$x = [R\ G\ B\ 1]$ (2)

$x = [R\ G\ B\ R^2\ RG\ RB\ G^2\ GB\ B^2]$ (3)

$x = [R\ G\ B\ R^2\ RG\ RB\ G^2\ GB\ B^2\ 1]$ (4)

$x = [R\ G\ B\ R^2\ RG\ RB\ G^2\ GB\ B^2\ R^3\ R^2G\ R^2B\ RG^2\ RGB\ RB^2\ G^3\ G^2B\ GB^2\ B^3]$ (5)

$x = [R\ G\ B\ R^2\ RG\ RB\ G^2\ GB\ B^2\ R^3\ R^2G\ R^2B\ RG^2\ RGB\ RB^2\ G^3\ G^2B\ GB^2\ B^3\ 1]$, (6)

where *R*, *G*, and *B* are the values of color components and $y = [R\ G\ B]$ is the vector of components from the color scale specification.

The values of RGB components for the feature vectors in this case is transferred from a standard RGB space to a linear RGB space by the following transformations:

$$\text{if color} < 0.04045\text{: linearColor} = \text{color} / 12.92$$

$$\text{else: linearColor} = \left(\frac{\text{color} + 0.055}{1.055}\right)^{2,4}$$

The estimates of transformation coefficients β are selected by solving the following system of equations:

$$\begin{bmatrix} y_1 \\ \cdots \\ y_{9\cdot 24} \end{bmatrix} = \begin{bmatrix} x_1 \\ \cdots \\ x_{9\cdot 24} \end{bmatrix} \begin{bmatrix} \beta_{11} & \cdots & \beta_{13} \\ \vdots & \ddots & \vdots \\ \beta_{n1} & \cdots & \beta_{n3} \end{bmatrix}$$

The resulting coefficients are then used to transform the color components of the pixels of the overall image.

To assess the differences between the color components of the initial and corrected images, we used a parameter, D_{col}, calculated as

$$\begin{bmatrix} \tilde{y}_1 \\ \cdots \\ \tilde{y}_{9\cdot 24} \end{bmatrix} = \begin{bmatrix} x_1 \\ \cdots \\ x_{9\cdot 24} \end{bmatrix} \begin{bmatrix} \tilde{\beta}_{11} & \cdots & \tilde{\beta}_{1n} \\ \vdots & \ddots & \vdots \\ \tilde{\beta}_{n1} & \cdots & \tilde{\beta}_{nn} \end{bmatrix}$$

$$D_{col} = 1 - \det[\tilde{\beta}]$$

Correspondingly, the feature vectors constructed analogously to *x*, rather than just colors, are used as $\tilde{y}$ and the resulting matrix $\tilde{\beta}$ is square. The closer the corrected color values to the initial ones, the closer is $\tilde{\beta}$ to unit matrix and, correspondingly, the closer is D_{col} to zero.

3. Supplementary tables

Table S1. Parameters determined by the application for recognizing spike shape.

Parameter	Measurement unit	Description
L	mm	Length of the broken line along the spike axis line
P	mm	Perimeter of spike contour without awns
E_a	mm^2	Area of spike contour without awns
A_a	mm^2	Total awn area
E_a/L^2	–	Ratio of spike area to its squared length
C	–	Circularity index, the ratio of the perimeter of the circle with the area equal to the area of spike contour to perimeter of the contour; this index shows the degree to which the contour shape is close to a circle and ranges from 0 to 1
R	–	Roundness, the ratio of spike contour area to the area of the circle with a diameter equal to the rotation axis of the contour (major axis)
Rg	–	Rugosity index, the ratio of contour perimeter to convex perimeter
S	–	Solidity index, the ratio of contour area to the area of its convex hull
x_{u1}	mm	Distance from the spike tip to projection B' of top B onto base AD
x_{u2}	mm	Distance from B' to projection C' of top C onto base AD
y_{u1}	mm	Distance from top B to its projection B' onto base AD
y_{u2}	mm	Distance from top C to its projection C' onto base AD
α_{u1}	Degrees	Inclination of edge AB relative to the base of the upper quadrilateral
α_{u2}	Degrees	Inclination of edge BC
α_{u3}	Degrees	Inclination of edge CD relative to the base of the upper quadrilateral
t_{u1}	–	Tangent of angle α_{u1}
t_{u2}	–	Tangent of angle α_{u2}
t_{u3}	–	Tangent of angle α_{u3}
S_{u1}	mm^2	Area of triangle ABB'
S_{u2}	mm^2	Area of trapezium $BB'C'C$
S_{u3}	mm^2	Area of triangle DCC'
S_u	mm^2	Area of upper quadrilateral
y_{um}	mm	Mean height of the upper quadrilateral
A_{Ix2}	mm	Asymmetry index for the lengths of segments
A_{Iy2}	mm	Asymmetry index for the heights of segments
A_{Ixy2}	mm	Total asymmetry index
Sections of spike contour (20 + 20 secti ons)	mm	Lengths of contour sections from the spike axial line: profile_1, profile_2, profile_3, …, profile_40
Radial spike model (360 length of intervals)	mm	Intervals from the center of mass to the nearest point of contour in 360 directions with a step of 1 degree starting from the major axis of the contour: radial_1, radial_2, radial_3, …, radial_360

Table S1 lists the parameters of the quadrilateral model only for the upper quadrilateral. The parameters for the lower quadrilateral correspond to those of the upper one: x_{b1}, x_{b2}, y_{b1}, y_{b2}, a_{b1}, a_{b2}, a_{b3}, t_{b1}, t_{b2}, t_{b3}, S_{b1}, S_{b2}, S_{b3}, S_{b}, and y_{bm}.

Table S2. Characteristics of the plants and spikes the images of which were used for training and testing the method for recognition of spike shape.

Species	Variety[1]	Catalog number[1]	Country[1]	Number of plants	Spike length (cm)[2]	Spike front width (cm)[2]	Spike side width (cm)[2]	Spikelet count[2]	Density index[2]	Shape type[3]	Awn type[4]
Amphyploid speltiforme	Aminov	—	Azerbaijan	9	9.04 ± 1.82	0.72 ± 0.19	0.73 ± 0.10	19.22 ± 3.56	20.25 ± 2.13	spelt: 9	awnless: 9
Triticum aestivum L.	—	k-1386	Tajikistan	18	7.43 ± 1.52	0.8 2± 0.18	0.74 ± 0.15	14.33±2.35	18.16±2.29	normal: 18	awnletted: 18
	ANK-23	—	Russia	17	6.60 ± 1.24	0.91 ± 0.19	0.70 ± 0.09	14.71±2.17	20.97±2.05	normal: 17	awnless: 10, awned: 7
	Babilo	—	Tajikistan	10	8.74 ± 1.08	1.01 ± 0.14	1.01 ± 0.14	17.30±1.16	18.80±1.59	normal: 10	awnless: 10
	Novosibirskaya 67	—	Russia	4	8.10 ± 2.49	0.70 ± 0.08	0.75 0.10	21.00 ± 3.65	26.28 ± 8.07	normal: 4	awnless: 4
	Triple Dirk D	AUS 90069	Australia	1	7.50 ± 0	1.30 ± 0	0.60 ± 0	15.00 ± 0	18.67 ± 0	normal: 1	awnless: 1
Triticum antiquorum Heer ex Udacz.	—	k-56397	Tajikistan	10	3.97 ± 0.43	0.69 ± 0.06	0.87 ± 0.05	17.60 1.17	42.42 ± 6.76	compact: 10	awnless: 10
	—	k-56398	Tajikistan	10	5.42 ± 0.34	0.77 ± 0.07	1.10 ± 0.08	19.20 ± 1.03	33.66 ± 2.40	compact: 10	awnless: 10
Triticum compactum Host	—	k1709	Tajikistan	19	5.36 ± 0.74	0.88 ± 0.15	1.12 ± 0.17	17.37 ± 3.35	30.36 ± 3.23	compact: 19	half-awned: 10, awned: 9
	—	k1711	Tajikistan	17	5.19 ± 0.63	0.91 ± 0.22	1.01 ± 0.24	15.35 ± 2.55	28.07 ± 6.22	compact: 17	awnletted: 10, awned: 7
	—	k1713	Tajikistan	18	5.34 ± 0.57	0.89 ± 0.21	1.04 ± 0.19	15.06 ± 2. 86	26.28 ± 4.47	compact: 18	awnletted: 18
	—	WAG 1326	Netherlands	1	4.00 ± 0	1.00 ± 0	1.50 ± 0	19.00 ± 0	45.00 ± 0	compact: 1	awned: 1
	—	WAG 8326	Netherlands	8	4.33 ± 0.37	0.83 ± 0.21	1.40 ± 0.23	19.88 ± 2.80	43.59 ± 5.06	compact: 8	awned: 8
Triticum macha Dekapr. et Menabde	—	—	Georgia	9	8.42 ± 1.04	0.62 ± 0.11	0.63 ± 0.10	18.78 ± 1.99	21.29 ± 2.70	spelt: 9	awnletted: 9
Triticum spelta L.	—	k-19092	Latvia	9	11.17 ± 1.35	0.63 ± 0.07	0.58 ± 0.07	15.56 ± 1.01	13.13 ± 1.00	spelt: 9	awnletted: 9
	—	k-53660	Tajikistan	1	9.40 ± 0	0.70 ± 0	0.60 0	14.00 0	13.83 ± 0	spelt: 1	awned: 1
	Rother Sommer Kolben	k-1731	Germany	8	8.15 ± 0.70	0.62 ± 0.08	0.63 ± 0.05	15.50 ± 1.69	17.79 ± 1.54	spelt: 8	awnless: 8

Triticum sphaerococcum Perc.	–	k-14976	Pakistan	9	3.72 ± 0.45	0.77 ± 0.16	0.87 ± 0.12	15.44 ± 1.01	39.26 ± 5.01	compact: 9	awnless: 9
	–	k-33750	Pakistan	10	3.46 ± 0.49	0.68 ± 0.13	0.71 ± 0.13	14.50 ± 1.08	39.58 ± 5.16	compact: 10	awnless: 10
Triticum yunnanense King ex S.L. Chen	KU 508	KU 508	China	1	10.90 ± 0	1.00 ± 0	0.90 ± 0	24.00 ± 0	21.10 ± 0	spelt: 1	awnless: 1
	KU 50-	KU 509	China	8	8.35 ± 0.59	0.70 ± 0.08	0.68 ± 0.10	16.13 ± 1.13	18.14 ± 1.14	spelt: 8	half-awned: 8
F2 Triple Dirk B × *Triticum yunnanense* KU506	–	–	–	52	8.17 ± 1.16	0.77 ± 0.17	0.87 ± 0.22	19.29 ± 2.82	22.78 ± 4.89	spelt: 22, normal: 22, compact: 8	awnless: 32, half-awned: 20

[1] (–), unavailable information.

[2] Data are shown as mean ± standard deviation.

[3] Numbers of occurrences of spikes of the corresponding types.

[4] Numbers of awns of the corresponding types.

Table S3. The effect of JPEG image quality on the accuracy of segmentation into three classes independently (ColorChecker, spike body, and awns) and the spike together with awns. The first column shows *QF* for different degrees of compression of the initial TIFF files. The other four columns show the Jaccard index, *J*, for comparisons of the corresponding image regions in the initial TIFF format and compressed JPEG variant for images of an awned spike (image no. 8731, Figure S4a and c) and an awnless spike (image no. 8733, Figure S4b and d).

Image no. 8731 (awned spike)				
JPEG quality	ColorChecker	Spike body	Awns	Spike (body_awns)
1	0.998	0.985	0.864	0.993
10	0.999	0.984	0.876	0.994
20	0.998	0.985	0.882	0.994
30	0.998	0.983	0.882	0.994
40	0.999	0.986	0.893	0.995
50	1	0.991	0.936	0.997
60	1	0.993	0.941	0.997
70	1	0.993	0.943	0.997
80	1	0.993	0.944	0.998
90	1	0.993	0.955	0.997
100	1	0.993	0.959	0.998
Image no. 8733 (awnless spike)				
JPEG Quality	ColorChecker	Spike body	Awns	Spike (body_awns)
1	0.998	0.986	0.74	0.997
10	0.999	0.984	0.736	0.998
20	0.999	0.986	0.753	0.999
30	0.999	0.988	0.779	0.998
40	0.999	0.988	0.787	0.999
50	0.998	0.991	0.837	0.998
60	0.998	0.992	0.847	0.997
70	1	0.993	0.873	1
80	1	0.993	0.86	1
90	1	0.994	0.894	1
100	1	0.995	0.909	1

Table S4. The performance measures for spike shape classification and density estimation for each of the five cross-validation iterations. Data shown for the 'table' and 'clip' protocols. The average values for performance measures is shown in two last columns. *F1* estimates for density prediction shown for two methods: linear regression (lr) and random forest (rf) without using predicted density values as additional parameter (lr, rf) and with this parameter (lr_density_pred, rf_density_pred).

Performance measure	Table/fold1	Clip/fold1	Table/fold2	Clip/fold2	Table/fold3	Clip/fold3	Table/fold4	Clip/fold4	Table/fold5	Clip/fold5	Average 'table'	Average 'clip'
Spike density estimation												
$MAE_{training}$	1.78	1.48	1.80	1.45	1.77	1.24	1.75	1.48	1.69	1.41	1.76	1.41
MAE_{test}	4.43	3.09	4.93	3.38	4.37	3.73	4.80	3.58	4.56	3.02	4.62	3.36
$MAPE_{training}$	7.14	6.10	7.28	6.17	7.34	5.17	6.96	6.13	6.94	5.74	7.13	5.86
$MAPE_{test}$	16.80	12.25	17.79	13.17	16.03	13.59	18.91	15.05	18.04	11.99	17.51	13.21
$R^2_{training}$	0.95	0.96	0.95	0.96	0.95	0.97	0.94	0.96	0.95	0.96	0.95	0.96
R^2_{test}	0.48	0.74	0.55	0.78	0.66	0.70	0.44	0.68	0.48	0.79	0.52	0.74
Spike shape classification												
F1 lr	0.77	0.85	0.75	0.87	0.76	0.73	0.72	0.76	0.83	0.87	0.77	0.82
F1 lr_density_pred	0.72	0.83	0.75	0.84	0.80	0.79	0.73	0.79	0.84	0.89	0.77	0.83
F1 rf	0.73	0.84	0.67	0.85	0.73	0.80	0.77	0.83	0.79	0.89	0.74	0.84
F1 rf_density_pred	0.76	0.83	0.72	0.85	0.80	0.85	0.76	0.83	0.84	0.88	0.78	0.85

4. Supplementary figures

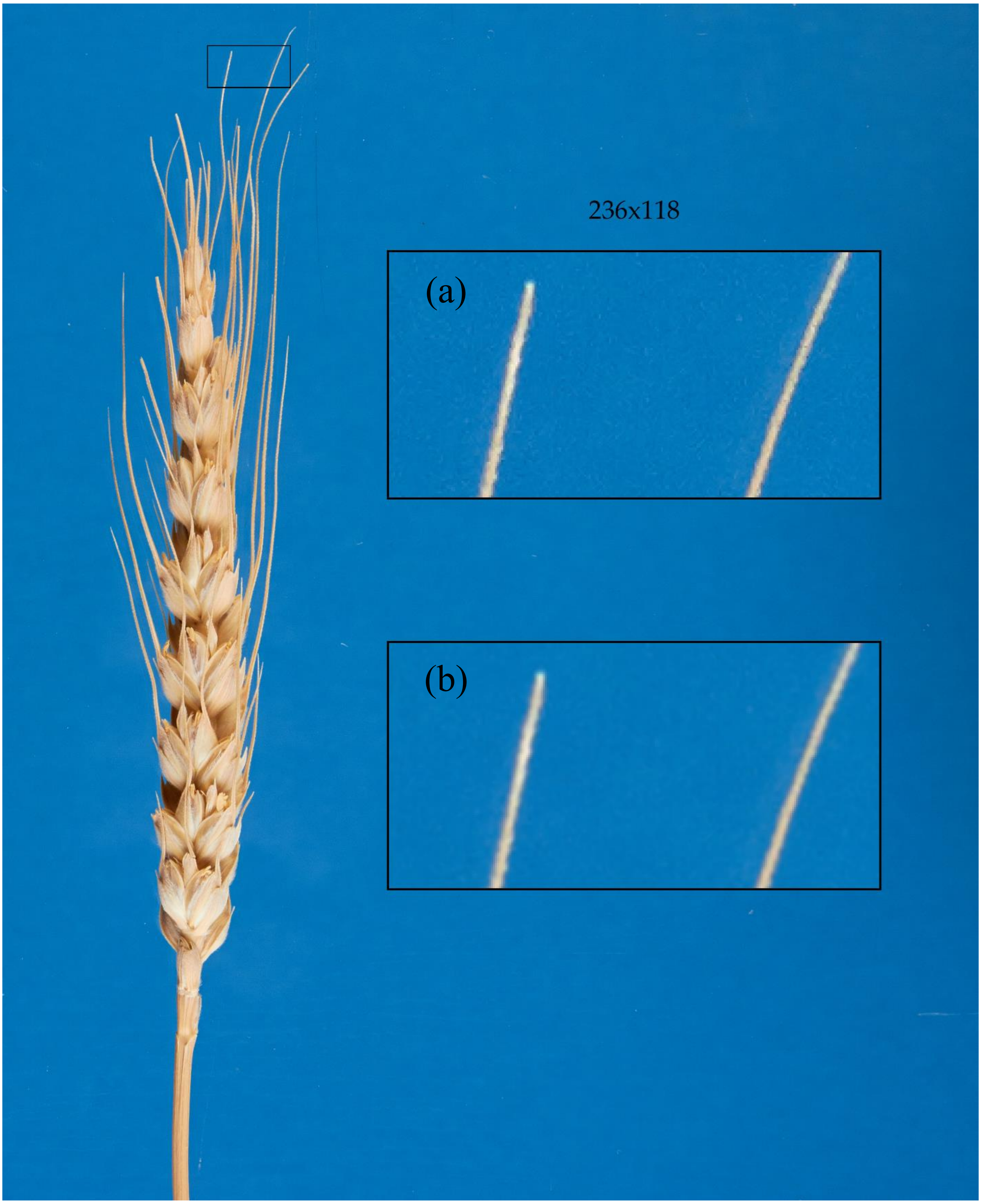

Figure S3. A zoomed-in fragment of the image illustrating the result of operation of the smoothing algorithm using a Gaussian filter with a 3 × 3 core: (a) a fragment of the initial image and (b) a fragment of the smoothed image.

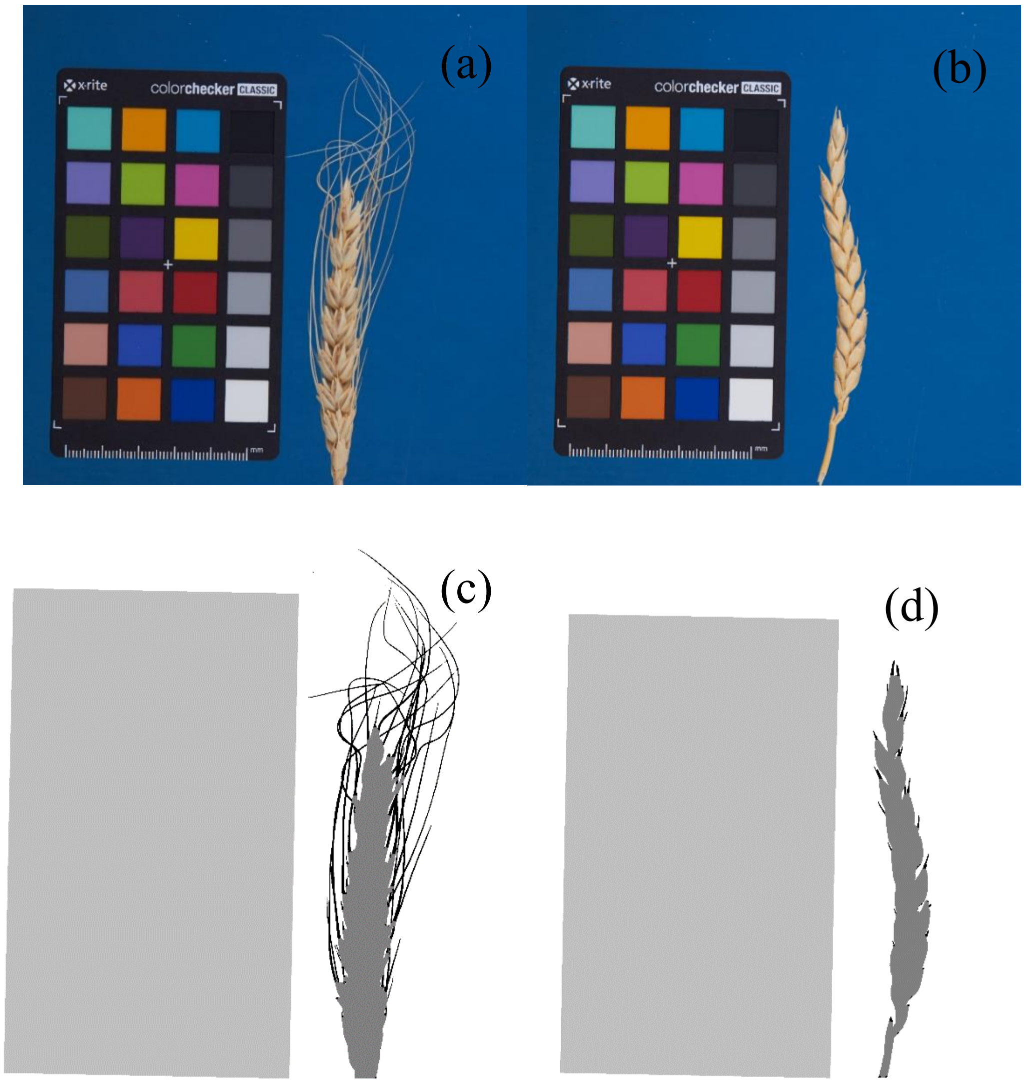

Figure S4. Images of spikes and the results of segmentation for two plants of the F_2 hybrids between common wheat Triple Dirk B and *Triticum yunnanense* with different awn types: (a) and (c) ID no. 8731 (awned); (b) and (d) ID no. 8733 (awnless). In segmented images, light gray corresponds to the ColorChecker; dark gray, to spike body; and black, to awns.

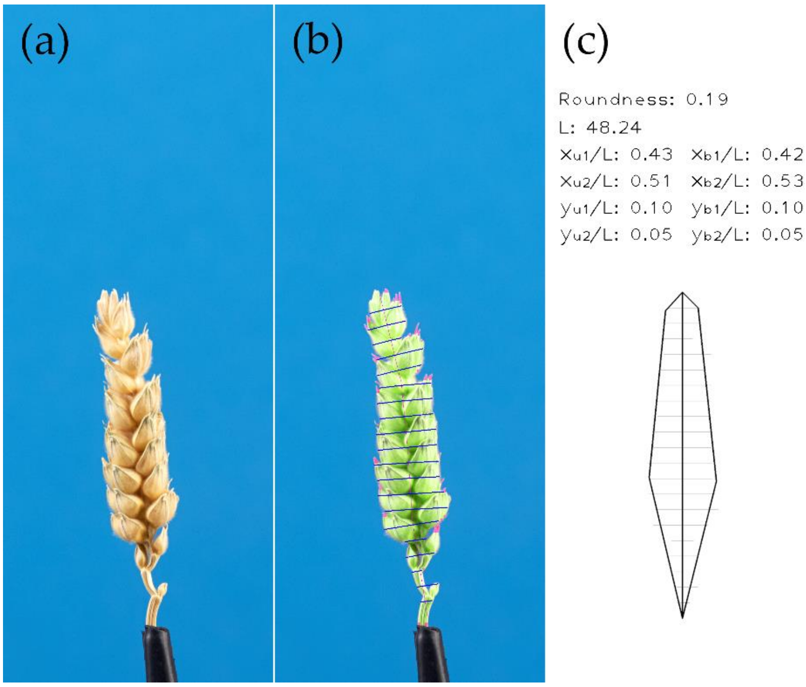

Figure S5. Stages of algorithm operation for compact spike type: (**a**) initial spike image; (**b**) the recognized spike body is highlighted with green; awn regions, with red; and sections, with blue; spike axis is denoted with red; and (**c**) Model of two adjacent quadrilaterals constructed based on extracted parameters.

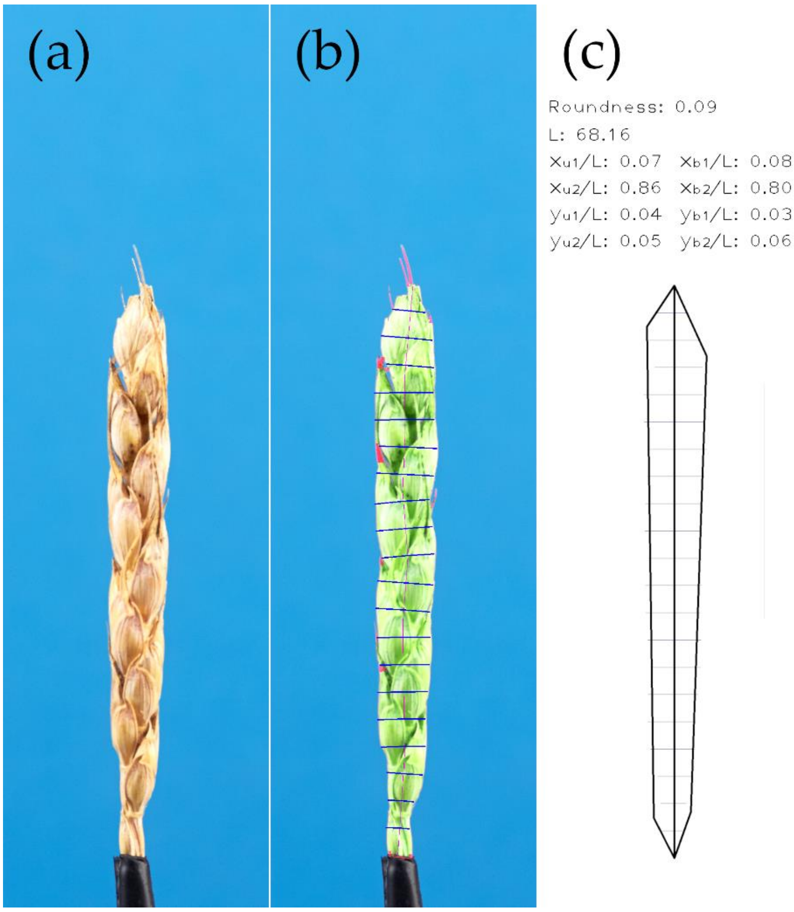

Figure S6. Stages of algorithm operation for normal spike types: (**a**) initial spike image; (**b**) the recognized spike body is highlighted with green; awn regions, with red; and sections, with blue; spike axis is denoted with red; and (**c**) Model of two adjacent quadrilaterals constructed based on extracted parameters.

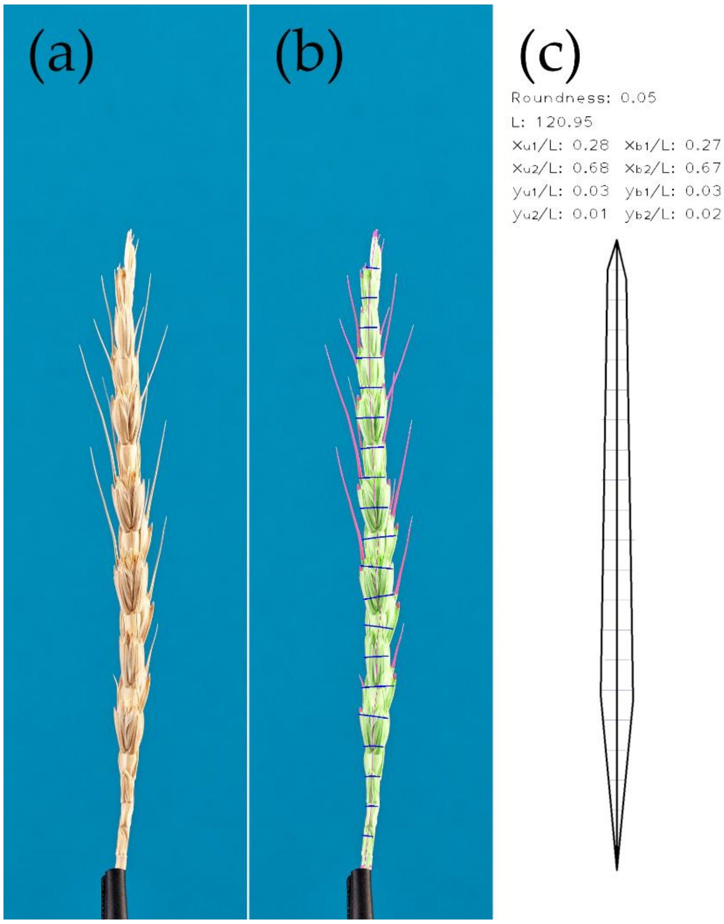

Figure S7. Stages of algorithm operation for spelt spike types: (**a**) initial spike image; (**b**) the recognized spike body is highlighted with green; awn regions, with red; and sections, with blue; spike axis is denoted with red; and (**c**) Model of two adjacent quadrilaterals constructed based on extracted parameters.

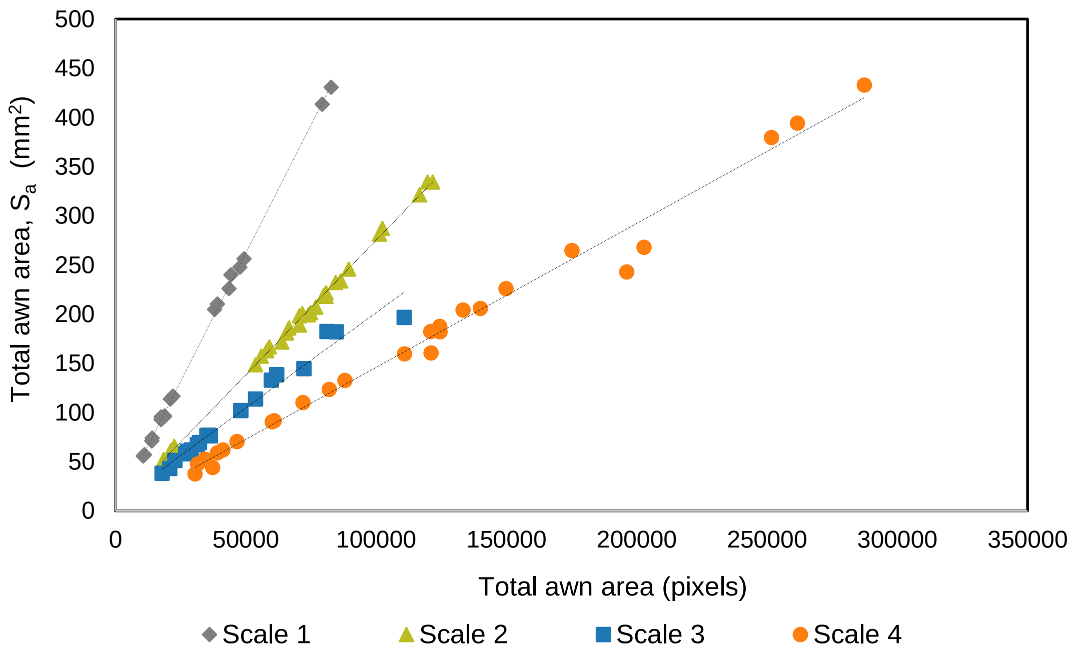

Figure S8. Ratio of the total pixels of awns to the total awn area (mm²) grouped according to the scale of the spatial resolution of the image from low resolution (scale 1) to high resolution (scale 4). The values of linear regression are α = 0.00526 for scale 1, α = 0.00277 for scale 2, α = 0.00213 for scale 3, and α = 0.00146 for scale 4.

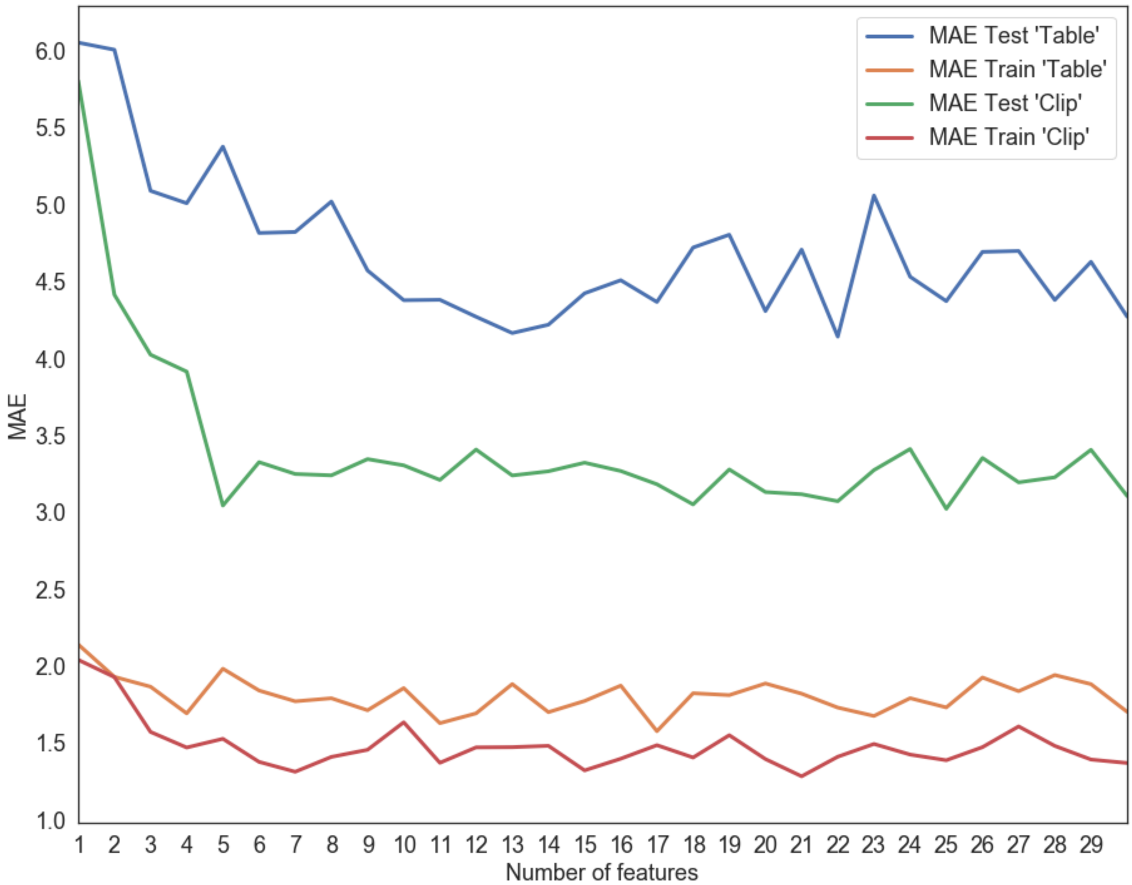

Figure S9. Dependence of the mean absolute error (MAE) in predicting spike density index on the number of best parameters used for training with random forest method.

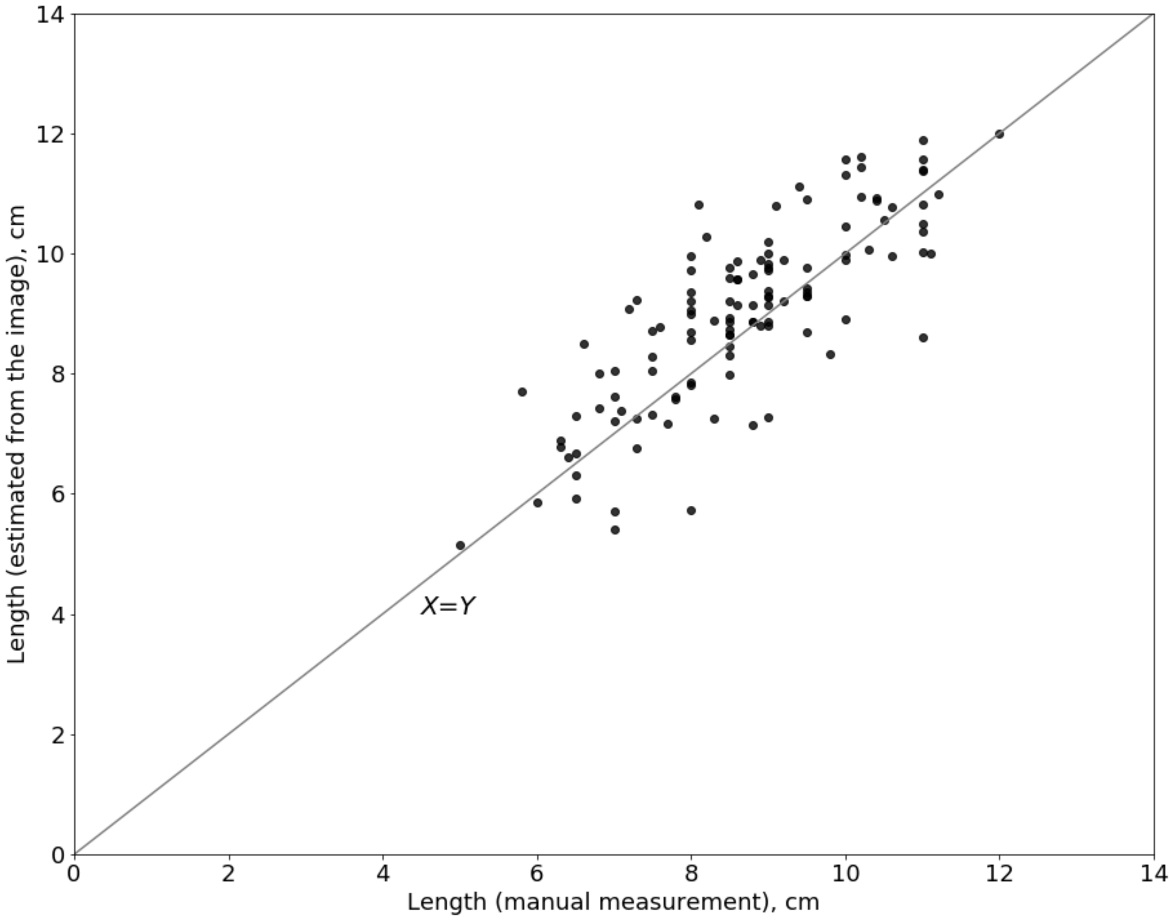

Figure S10. Scatterplot diagram for the main spike length for Triple Dirk B × K U506 F_2 hybrid plants estimated manually (X axis) and from the 2D image analysis (Y axis). The solid line is Y=X line.

Figure S11. A zoomed-in fragment of the image illustrating the result of operation of the algorithm for segmenting spike awns.

References

1. Kaehler, A.; Bradski, G. Learning OpenCV 3: computer vision in C++ with the OpenCV library. *O'Reilly Media, Inc.* **2016**.
2. Quintana, J.; Garcia, R.; Neumann, L.A novel method for color correction in epiluminescence microscopy. *Comput. Med. Imag. Grap.* **2011**, 35 (7-8), 646-652 [CrossRef] [PubMed].